†Work supported in part by the National Science Foundation and by the Advanced Research Projects Agency.

*Present address: Physics Department, McMaster University, Hamilton, Ontario, Canada.

[1]A. R. Miedema, H. van Kempen, and W. J. Huiskamp, Physica 29, 1266 (1963).

[2]H. Abe, K. Ono, I. Hayashi, J. Shimada, and K. Iwanaga, J. Phys. Soc. Japan 9, 814 (1954).

[3]I. Svare, Ph. D. thesis, Harvard University, 1962 (unpublished); I Svare and G. Seidel, Cruft Laboratory Technical Report No. 378, 1962 (unpublished).

[4]G. Seidel and S. H. Choh, Bull. Am. Phys. Soc. 11, 186 (1966).

[5]K. Tomita, in Proceedings of the International Conference on Theoretical Physics, Kyoto and Tokyo, September, 1953 (Science Council of Japan, Tokyo, 1954), p. 800.

[6]A. J. Henderson, Jr., and R. N. Rogers, Phys. Rev. 152, 218 (1966).

[7]R. N. Rogers (private communication) indicates that the value of the exchange estimated in Ref. 6 of 0.24 °K is in error by a factor of 2.

[8]A. R. Miedema, R. F. Wielinga, and W. J. Huiskamp, Physica 31, 1585 (1965).

[9]D. W. Wood and N. W. Dalton, Proc. Phys. Soc. (London) 87, 755 (1966).

[10]H. Abe, J. Phys. Soc. Japan 16, 836 (1961).

[11]T. Okuda and M. Date, J. Phys. Soc. Japan 28, 308 (1970).

[12]See R. W. Wyckoff, Crystal Structures (Interscience, New York, 1948), Vol. III.

[13]R. Chidambaram, Q. O. Navarro, A. Garcia, K. Linggoatmodjo, L. Shi-Chien, and I. Suh, J. Korean Phys. Soc. 2, 13 (1969).

[14]H. Suzuki and T. Watanabe, Phys. Letters 26A, 103 (1967).

[15]B. Bleaney, K. D. Bowers, and M, H. L. Pryce, Proc Roy. Soc. (London) A228, 166 (1955).

[16]M. C. M. O'Brien, Proc. Roy. Soc. (London) A281, 323 (1964).

[17]See M. D. Sturge, in Solid State Physics, edited by F. Seitz, D. Turnbull, and H. Ehrenreich (Academic, New York, 1967), Vol. 20, p. 91.

[18]P. W. Anderson and P. R. Weiss, Rev. Mod. Phys. 25, 269 (1953).

[19]P. W. Anderson, J. Phys. Soc. Japan 9, 316 (1954).

[20]J. E. Gulley, B. G. Silbernagel, and V. Jaccarino, J. Appl. Phys. 40, 1318 (1969).

[21]T. R. Reddy and R. Srinivasan, Phys. Letters 22, 143 (1966).

[22]T. Moriya, Phys. Rev. 120, 91 (1960).

[23]J. W. Philp and E. D. Adams, J. Low Temp. Phys. (to be published).

[24]S. H. Choh and C. V. Stager, Can. J. Phys. (to be published).

[25]H. Bayer, Z. Physik 130, 227 (1951).

[26]K. R. Jeffrey and R. L. Armstrong, Phys. Rev. 174, 359 (1968).

Inelastic Neutron Scattering from Single-Domain BaTiO₃†

G. Shirane, J. D. Axe, and J. Harada

Brookhaven National Laboratory, Upton, New York 11973

and

A. Linz

Center for Materials Science and Engineering, Massachusetts Institute of Technology, Cambridge, Massachusetts 02139

(Received 4 May 1970)

The lattice dynamics of tetragonal BaTiO₃ have been investigated by inelastic neutron scattering from a single-domain crystal. Measurements were carried out on two projections, $(hk0)$ and $(h0l)$; the study revealed extreme anisotropy in energy and damping of the soft optic mode, depending upon the polarization vector $\vec{e}$. The lowest transverse optic branch with the wave vector $\vec{q} \parallel [110]$ and $\vec{e} \parallel [1\bar{1}0]$ shows well-defined phonons except for small q values (< 0.05 Å^{-1}), where they become overdamped. The soft-mode energy increases rapidly with q and extrapolates back to 4.5 meV at the zone center, in agreement with the previous Raman measurements. On the other hand, the soft modes with $\vec{e} \parallel [100]$ (with $\vec{q} \parallel [010]$ or $[001]$) have unusually low energies and high damping constants for the entire zone. They cross over the acoustic branches, resulting in marked anomalies for the latter. The present study establishes the validity of the soft-mode model for ferroelectricity in BaTiO₃, as was the case for SrTiO₃. The important feature for BaTiO₃ is the greatly enhanced polarization correlation along the [100] direction compared with other perovskites.

I. INTRODUCTION

Barium titanate has long been considered as the prototype of displacive ferroelectrics. It crystallizes in a simple perovskite structure, and its properties through the Curie temperature at 130 °C have been thoroughly investigated. There is, however, one important characteristic of this ferroelectric yet to be clarified, namely, the lattice dynamical aspect of the transition in terms of the soft optic mode.

The soft-mode behavior in other perovskite-type incipient ferroelectrics, such as $SrTiO_3$ and $KTaO_3$, has now been well established. According to Cochran,[1] the soft-mode energy $\hbar\omega_0$ is expected to follow the relation

$$(\hbar\omega_0)^2 = K/\epsilon \cong A(T - T_0) . \qquad (1)$$

This was confirmed for $SrTiO_3$ and $KTaO_3$ by accurate measurements by Raman[2] and neutron[3-5]-scattering techniques. Recently, $PbTiO_3$ was investigated by neutron scattering[6]; well-defined soft modes were observed in the ferroelectric as well as in the paraelectric phase. For these crystals, the lowest transverse optic branch has been measured for the entire Brillouin zone by the neutron-scattering technique. For example, the dispersion of the soft-mode branch in $SrTiO_3$ is shown in Fig. 1(a) for two principal crystallographic directions.[4] Anisotropy of the energy is not great, and the phonons are well defined at all temperatures and their linewidth has been measured accurately.[2,4]

As for $BaTiO_3$, a satisfactory picture has not yet emerged with respect to the exact characteristics of the soft mode, especially in its $\vec{q}$ dependence. In the cubic phase above $T_c = 130\,°C$, the infrared measurements by Barker[7] reported an overdamped

FIG. 1. Soft optic mode along two principal directions. The data for $SrTiO_3$ were obtained at $4\,°K$ by Yamada and Shirane (Ref. 4). The ones for $BaTiO_3$ are drawn schematically as Hüller's theoretical model predicted (Ref. 11).

mode at $q = 0$. The recent neutron study[8] showed the quasielastic scattering with a strong-intensity anisotropy in the reciprocal lattice. This indicates that the correlation of the polarization fluctuation is along [100] in agreement with the previous observation of diffuse scattering by electron and x-ray diffraction.[9,10] There is, moreover, some controversy concerning the origin of this diffuse scattering. Comes et al.[10] postulate that the low-temperature rhombohedral phase of $BaTiO_3$ is the only perfectly ordered structure. The higher-symmetry orthorhombic, tetragonal, and cubic phases are disordered structures resulting from several possible orientations of $BaTiO_3$ units along different [111] directions. These orientations are thought to be highly correlated into a chainlike structure giving rise to the observed anisotropy of diffuse scattering. On the other hand, Harada and Honjo[9] proposed that the only disorder necessary to explain such diffuse scattering is the dynamic disorder due to low-energy optical phonons. If we adopt this view, the strong anisotropy in the diffuse scattering must result from a strong anisotropy in an optic phonon-dispersion surface[11] such as is shown schematically in Fig. 1(b). Our measurements will provide crucial experimental evidence on this point.

This paper reports the first neutron-scattering experiment on single-domain $BaTiO_3$ crystals in the ferroelectric state. Large single crystals of high purity $BaTiO_3$ can now be grown by a top-seeded solution method.[12] Single-domain crystals of this type were used in recent Raman scattering[13] and dielectric[14] measurements, as well as in the present neutron studies. The clamped dielectric constants at $25\,°C$ were reported as $\epsilon_d = 2300$ and $\epsilon_c = 80$.

The Raman spectrum of tetragonal $BaTiO_3$ was studied by DiDomenico et al.[13] They reported that the soft E mode is overdamped with $\hbar\omega_1 = 4.4$ meV and $\Gamma/2\omega_1 = 1.1$ at $25\,°C$. This is in substantial agreement with the infrared study by Barker[7] and consistent with the Lyddane-Sachs-Teller relation. On the other hand, other Raman measurements[15,16] assigned the E mode at 1.5 meV.

It is of great interest to investigate the behavior of the soft mode at higher q values, in particular, its dependence on the direction of the polarization vector $\vec{e}$. The x-ray studies[9,10] have already shown that the diffuse scattering forms a set of planes perpendicular to the tetragonal [100] axis. Inelastic neutron scattering, however, is the only tool available at present to measure directly the excitation energies over the entire Brillouin zone.

II. EXPERIMENTAL

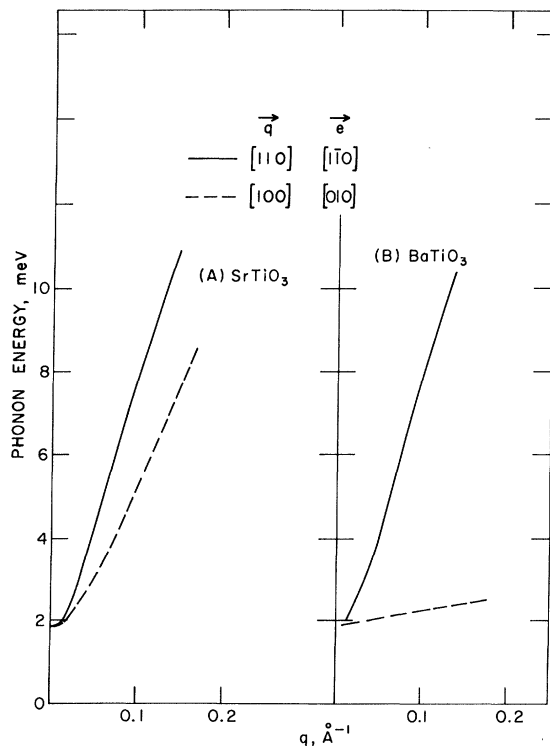Measurements were carried out on a single-domain crystal of tetragonal $BaTiO_3$. The crystal

was grown from the melt by the technique previously described.[12] The most difficult part of the crystal preparation was the poling through the Curie temperature in order to produce a large enough single-domain crystal for inelastic neutron measurements. This poling process was kindly facilitated by Dr. M. DiDomenico of Bell Telephone Laboratories. After a few crystals were cracked during the process, a single-domain crystal was successfully prepared. It has a dimension of $5 \times 5 \times 4$ mm^3.

Neutron measurements at 22 °C were carried out at the Brookhaven High-Flux Beam Reactor using a triple-axis spectrometer and the constant-Q scan. In order to compensate for the small size of the crystal, an effort was made to use neutrons efficiently and to reduce the background. Pyrolytic graphite crystals, provided by Union Carbide Corporation, were used as both monochromator and analyzer. These have a mosaic spread [full width at half-maximum (FWHM)] of 0.4 deg and are extremely efficient for the neutron energy range used for the present study, 40–10 meV. Most of the data were collected with the incoming energy $E_0 = 38$ meV and beam collimation of 20' before and after the scattering. Some measurements at small q were carried out with $E_0 = 14$ meV.

The crystal has a narrow mosaic of less than 1'. Therefore, the measurements at small q values were not limited by crystal mosaic, but by the resolution of the spectrometer. The two areas in the $\hbar\omega$-q space are beyond reach of the present study: The first is any phonon with energy higher than 25 meV, and the second is a narrow region at the zone center with $q < 0.04$ Å^{-1} and $\hbar\omega < 4$ meV. The latter requires a lower neutron energy or a tighter collimation than our present intensity compromise permits.

III. SOFT OPTIC MODES

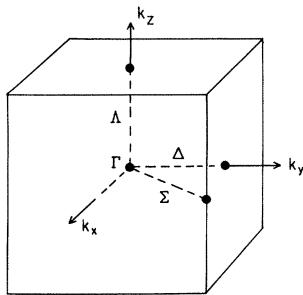Inelastic neutron-scattering measurements were

FIG. 2. Brillouin zone for a simple tetragonal lattice showing the notation used for special symmetry directions and for irreducible representations for the groups of the wave vectors corresponding to these directions. The z axis is the fourfold axis.

TABLE I. Symmetry properties of phonon modes in tetragonal BaTiO$_3$.[a]

Point group/ irreducible rep'ns	$\vec{q}$	Compatibility cubic $\rightarrow$ tetragonal
Δ	$(\zeta, 0, 0)$	Δ_1, $\Delta_2 \rightarrow \Delta_1$
$\chi^R(\Delta) = 10\Delta_1 + 5\Delta_2$		$\Delta_5 \rightarrow \Delta_1 + \Delta_2$
Σ	$(\zeta, \zeta, 0)$	Σ_1, $\Sigma_4 \rightarrow \Sigma_1$
$\chi^R(\Sigma) = 9\Sigma_1 + 6\Sigma_2$		Σ_2, $\Sigma_3 \rightarrow \Sigma_2$
Λ	$(0, 0, \zeta)$	$\Lambda_1 \rightarrow \Lambda_1$
$\chi^R(\Lambda) = 4\Lambda_1 + \Lambda_2 + 5\Lambda_5$		$\Lambda_2 \rightarrow \Lambda_2$
		$\Lambda_5 \rightarrow \Lambda_5$
Γ	$(0, 0, 0)$	$\Gamma_{15} \rightarrow \Gamma_1 + \Gamma_5$
$\chi^R(\Gamma) = 4\Gamma_1 + \Gamma_2 + 5\Gamma_5$		$\Gamma_{25} \rightarrow \Gamma_2 + \Gamma_5$
$\quad = 4A_1 + B_1 + 5E$		

[a]Notation for the cubic representations is that of Ref. 3. For Γ the widely used "chemical" notation is included.

carried out in the four symmetry directions in reciprocal space shown in Fig. 2. Table I summarizes the symmetry classification of the normal modes by decomposition of a reducible representation $\chi_R(G_t)$ generated by Cartesian displacements. G_t is the group of the wave vector appropriate to the tetragonal C_{4v}^1 space group. Compatibility relations between the groups $G_c \rightarrow G_t$ are also shown where G_c is the group appropriate for the O_h^1 symmetry of the cubic high-temperature form. The latter not only shows immediately the splittings to be expected as a result of the transformation but also allows a complete symmetry description of the modes through contact with the results of Ref. 3, to which interested readers should refer. Vectors in the reciprocal space are represented as $(\zeta_1, \zeta_2, \zeta_3)$, where the ζ_i are in units of the reciprocal-lattice vectors ($a^* = b^* = 1.574$ Å^{-1}, $c^* = 1.557$ Å^{-1} at 22 °C).

A. Soft Mode with $\vec{e} \parallel [1\bar{1}0]$

The dispersion relations for the lowest Σ_2 phonons ($\vec{q} \parallel [110]$ and $\vec{e} \parallel [1\bar{1}0]$) are shown in Fig. 3. The initial slope on the acoustic branch is calculated from the elastic constants.[17] A typical phonon profile is shown in Fig. 4(a) in comparison with

TABLE II. Four phonon types investigated for tetragonal BaTiO$_3$, specified by wave vector $\vec{q}$ and polarization vector $\vec{e}$. Initial slope of the transverse acoustic branch was calculated from the elastic constants (Ref. 17).

q	e	Neutron data taken around	Initial TA slope (meV Å)
Σ_2	[110]	[1$\bar{1}$0]	(220)	1.86
Δ_2	[010]	[100]	(200) (400)	2.85
Λ_5	[001]	[100]	(200) (400)	1.97
Δ_1	[100]	~[001]	(002) (004)	2.41

broad profiles [Fig. 4(b)] in the Λ_5 branch, which
were studied in the same projection $(H, K, 0)$. We
note a few important characteristics in Fig. 4(a):
(a) The large cross-section around $\Delta E = 0$ is due
to the elastic incoherent scattering of Ba and Ti.
(b) The TA mode is extremely sharp due to an
ideal focusing condition.[18] This sharp line serves
as a convenient check of instrumental resolution
and mosaic spread of the crystal and permits us
to put an upper limit of phonon linewidth (FWHM)
as 0.2 meV. (c) Most important is the lack of any
indication of a TO made in the energy range covered,
in contrast to the case shown in Fig. 4(b).

The TO branch was clearly observed by constant
E scans as shown in Fig. 5. This particular type
of scanning is dictated by a steep slope of the TO
mode in relation to the slope of the neutron probe
itself. This resolution problem is also the cause
of entirely different line shapes for the TA and
TO modes; the apparent broadness of the TO mode
is not due to intrinsic line broadening. With prop-
er consideration of the resolution and the anisot-

FIG. 4. Two examples of phonon profiles obtained in
the $(H, K, 0)$ plane. The peaks at $\Delta E = 0$ come from in-
coherent scattering of Ba and Ti; their width is determined
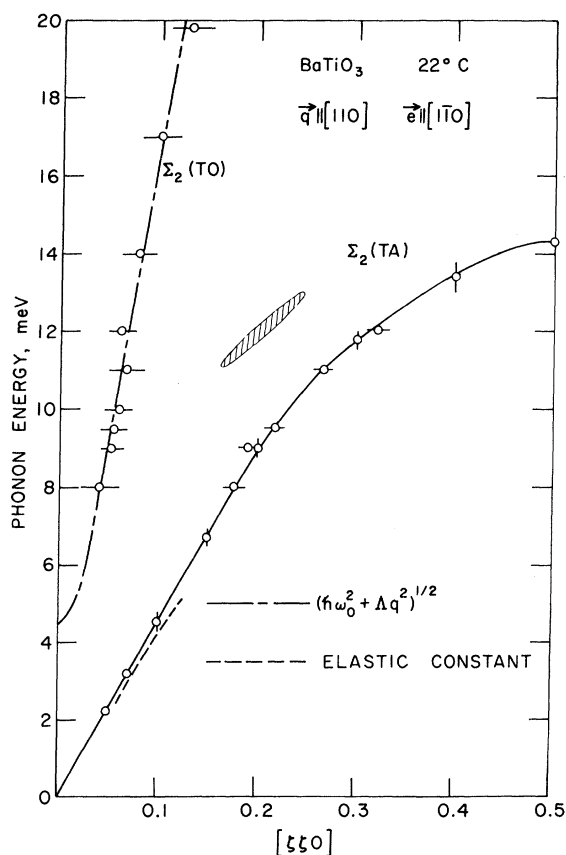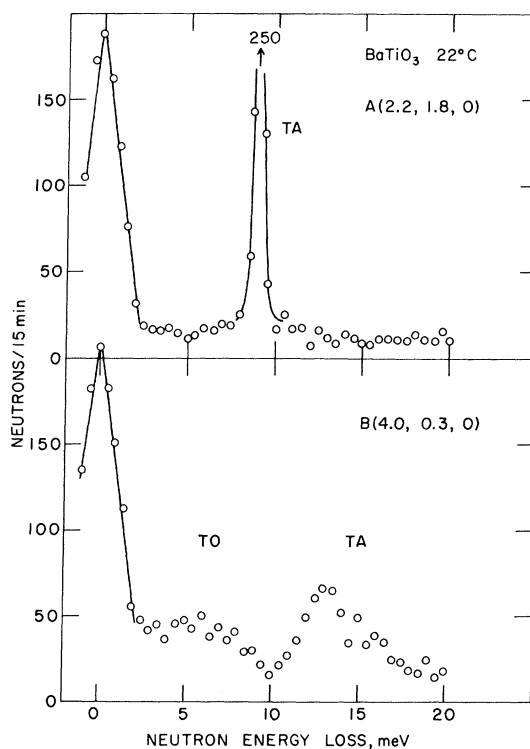by energy resolution of the instrument.

FIG. 3. Transverse branches with $\vec{e} \parallel [1\bar{1}0]$. The
chained curve for the TO branch was calculated as ex-
plained in the text. The size of neutron probe for E_0
$= 38$ meV is illustrated as an inserted ellipse.

ropy of the dispersion alone, one can satisfactorily
account for the observed line shape and intensity.
The details of this consideration will be described
in a forthcoming paper[19] to deal with the cubic
phase of $BaTiO_3$. Thus, we can conclude that the
TO mode with $\vec{e} \parallel [1\bar{1}0]$ is well defined (not over-
damped) except for the narrow range with $\zeta < 0.05$
and $\hbar\omega < 8$ meV. In this region, it was not possible
to obtain a clear picture due to the large instru-
mental resolution and, probably, due to over-
damping of the TO mode.

Phonon energy $\hbar\omega_1$ for TO modes can be ex-
pressed with good approximation[20] for small q as

$$(\hbar\omega_1)^2 = (\hbar\omega_0)^2 + \Lambda q^2 \ , \tag{2}$$

where $\hbar\omega_0$ is soft-mode energy at $q = 0$, and Λ is a
constant for a given $\vec{q}$ direction. The chained line
in Fig. 3 is drawn with $\hbar\omega_0 = 4.5$ meV and $\Lambda = 5100$
$(\text{meV})^2 \text{Å}^2$. This value $\hbar\omega_0$ has a large uncertainty
due to wide extrapolation and probably reliable
only with ± 1 meV. This value is in agreement with
the Raman data.[13]

A comparison of Fig. 3 with 1(a) shows that
the soft TO more with $\vec{e} \parallel [1\bar{1}0]$ in $BaTiO_3$ behaves
in a similar way to that of $SrTiO_3$, though the lat-
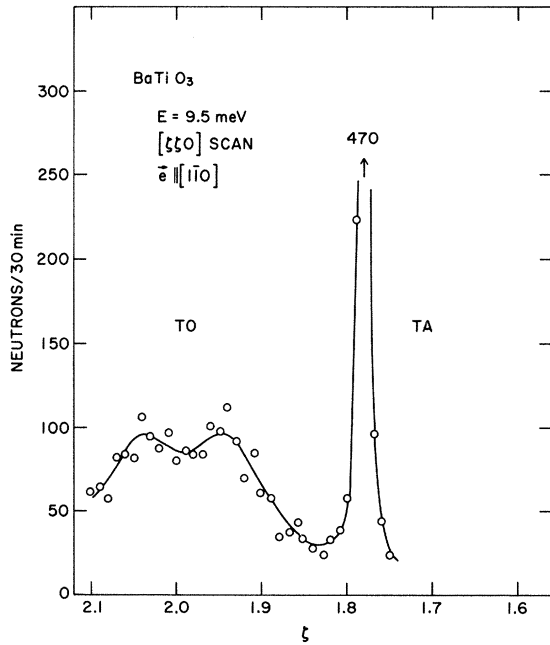ter's slope is not as steep. We may also recall

FIG. 5. Constant E scan along [110] direction. This scan corresponds to the horizontal line at $\Delta E = 9.5$ meV in Fig. 3. The different line shapes for TO and TA can be explained by dispersion slopes without invoking a broadening for TO.

that this steep slope for $\vec{e} \parallel [1\bar{1}0]$ is the basic conclusion from Hüller's model[11] of cubic $BaTiO_3$. It is important to recognize that this is the first observation of well-behaved soft modes in $BaTiO_3$,
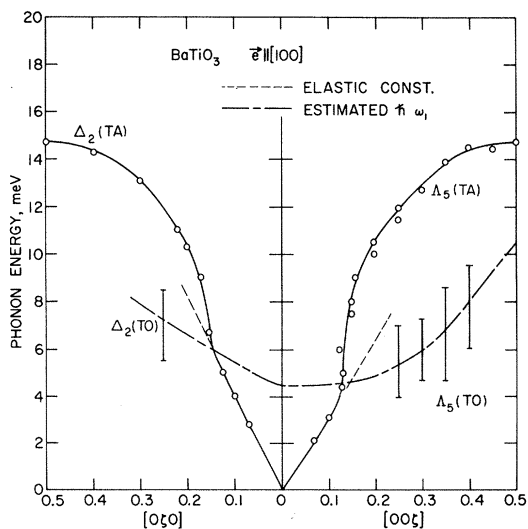

FIG. 6. Transverse branches with $\vec{e} \parallel [100]$. The chained line represents estimated undamped energy $\hbar\omega_1$ as explained in the text.
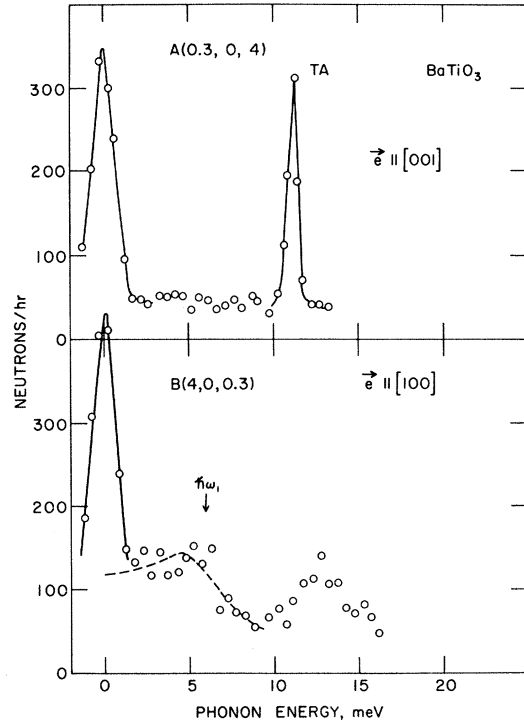

FIG. 7. Two examples of phonon profiles observed in the $(H, 0, L)$ plane. The broken line in B was calculated with $\hbar\omega_1 = 6$ meV and $\Gamma/2\omega_1 = 0.5$ in Eq. (3) of the text.

namely, underdamped and *above* the TA branch.

B. Soft Mode with $\vec{e} \parallel [100]$

We now examine the behavior of soft modes of type Δ_2 and Λ_5. Both mode types have polarization vectors $\vec{e}$ parallel to [100]. The dispersion relation is shown in Fig. 6, and examples of observed cross sections are given in Figs. 4(b) and 7(b). The TO modes here show entirely different characteristics from those with $\vec{e} \parallel [1\bar{1}0]$. The soft modes have low energy for the entire zone, and they cross over the TA branch. Since both transverse branches belong to the same representation, they should be drawn without touching each other. We have chosen to draw the dispersion as shown, since high damping of the TO mode with small q values prevented the direct observation of the underdamped mode frequencies.

Observed phonon profiles of TO modes were analyzed by using the damped simple-harmonic-oscillator formula with undamped energy $\hbar\omega_1$ and frequency-independent damping constant Γ,

$$F = \frac{\Gamma}{(\omega_1^2 - \omega^2)^2 + \omega^2\Gamma^2} \quad . \tag{3}$$

An example of the fit with experimental data at $\zeta = 0.3$ is shown in Fig. 7(b) by a broken line, cal-

culated with parameters $\hbar\omega_1 = 6$ meV, $\Gamma/2\omega_1 = 0.5$. Estimated $\hbar\omega_1$ is shown in Fig. 6 as the chained line. The value of $\Gamma/2\omega_1$ tends to increase with decreasing q value.

The observed line shapes of the TA mode in Figs. 4(b) and 7(b) clearly indicate line broadening in these phonons. This is probably due to a mode coupling with the crossed-over TO mode. Despite this modest line broadening, peak positions of the TA branch were identified uniquely for the entire zone. The most striking feature of the TA branch in Fig. 6 is the steep rise around $\zeta = 0.15$.

C. Transverse Modes with $\vec{e} \parallel [001]$

Dispersion curves for the lowest-lying phonon of symmetry Δ_1 are shown in Fig. 8. (The only symmetry requirement is that the mode eigenvectors be invariant to reflection in the x-z plane, and the modes are thus not strictly transverse or longitudinal, although we will continue to use this approximate description.) The lowest TO mode at $|q| \rightarrow 0$ contributes to the "hard" dielectric response $\epsilon_c = 80$, and must therefore be a considerably higher frequency than the soft TO modes with $\vec{e} \perp c$. The lowest phonon of this type observed was at 22 meV (178 cm^{-1}) in agreement with the lowest "sharp" $\Gamma_1(=A_1)$ mode observed in Raman scattering.[13,15,16,21] We find no evidence for a heavily damped excitation of this type below 22 meV assigned by DiDomenico et al.[13] to the lowest Γ_1 mode, although it is impossible to rule out its presence from our data.

The slope of the Δ_1(TA) mode as $|q| \rightarrow 0$ is worthy of some comment. Although both Λ_5(TA) and Δ_1 (TA) should have limiting slopes proportional to $(C_{44})^{1/2}$, in the former case C_{44}^E is appropriate while C_{44}^D is correct for the latter. This is readily established from the general acoustic wave solutions given, for example, by Hutson and White,[22] but the following qualitative lattice dynamical picture is equally instructive. Several authors[1,23,24] have discussed the internal strain and piezoelectric contributions to the elastic constants in terms of harmonic coupling proportional to $|q|$ of "bare" acoustic modes (pure translations) and $q = 0$ optic modes. In the case of modes propagating along Λ, the symmetry of the piezoelectric coefficient concerned (e_{61}) is such as to couple Λ_5(TA) (S_6 strain) with Λ_5(TO) (P_1 polarization). As there is no change bunching associated with the transverse-polarization wave ($\nabla \cdot \vec{P}_T = 0$), the appropriate electrical boundary condition is $E = 0$. On the other hand, along Δ the same e_{61} couples Δ_1(TA) with Δ_1(LO) modes. Associated with the longitudinal polarization there is a macroscopic electric field $\vec{E}_L = - 4\pi\vec{P}_L$, and the appropriate electrical boundary conditions are $\vec{D} = \vec{E} + 4\pi\vec{P} = 0$. (There is interaction between Δ_1(TA) and Δ_1(TO) as well, but it is quadratic or higher in $|q|$ and thus does not affect the limiting slope.[20])
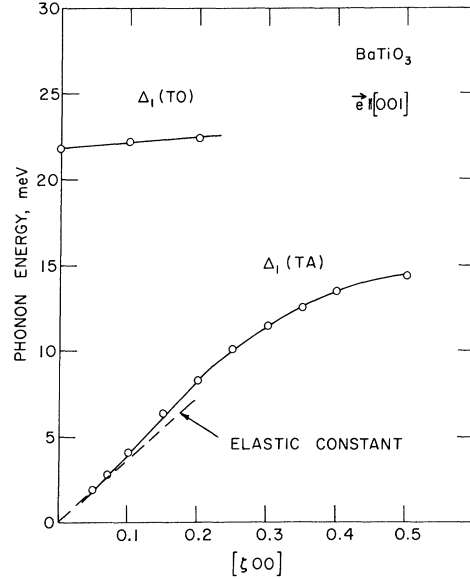

FIG. 8. Transverse branches with $\vec{e} \parallel [001]$. The dielectric constant $\epsilon_c = 80$ is considerably smaller than ϵ_a in the tetragonal phase.

IV. DISCUSSION

With regard to the nature of the phase transformation in BaTiO$_3$, the present experiments completely confirm its dynamical nature; i.e., we can clearly associate the transformation with an instability in the excitation spectrum. The question of the exact nature of the soft excitations is somewhat more subtle. However, in directions investigated along which the soft branch is not overdamped (all directions except those with $\vec{e}[100]$ and $\vec{q}[010]$ or $[001]$), there is every reason to believe that a quasiharmonic phonon description is appropriate. It is also clear from Fig. 7(b), for example, that along those remaining reciprocal-lattice directions for which strong x-ray diffuse scattering occurs, there is an appreciable damped inelastic component arising from the soft optic branch. (This inelasticity cannot, of course, be sensed from x-ray measurements.) It is not entirely clear that for these relatively few heavily damped modes that a phonon description is most appropriate. Cochran[25] has argued that the magnitude of the Curie constant is more compatible with a phononlike description of the critical condensing modes (as opposed to tunneling excitations between multiple potential minima).

Both the anomalous width and the unusual dispersion present for TA phonons of type Δ_2 and Λ_5 are undoubtedly due to coupling of acoustic and optic excitations. Piezoelectric coupling (proportional to $|q|$) has been discussed by Dvorak[23] and

higher-order coupling by Axe *et al.*[20] Neither of these treatments includes damping effects which are certainly extremely important in discussing the dynamical as opposed to the limiting static behavior of $BaTiO_3$, so that a quantitative comparison is not possible at the present time.

The present observations on tetragonal $BaTiO_3$ have raised further interesting questions concerning the cubic phase as well. For example, the extreme anisotropy of the soft phonon branch must persist into the cubic phase if this is the origin of the diffuse x-ray scattering. Due to larger sample size, it is also possible in the cubic phase to reach more

definite conclusions concerning the central question of the frequency distribution of the diffuse scattering, particularly with regard to the possibility of a large static component. These topics form the basis of a forthcoming paper.[19]

†Work performed under the auspices of the U. S. Atomic Energy Commission and Advanced Research Project Agency.

[1]W. Cochran, Advan. Phys. 9, 387 (1960); 10, 401 (1961).

[2]P. A. Fleury and J. M. Worlock, Phys. Rev. 174, 613 (1968).

[3]R. A. Cowley, Phys. Rev. 134, A981 (1964).

[4]Y. Yamada and G. Shirane, J. Phys. Soc. Japan 26, 396 (1969).

[5]G. Shirane, R. Nathans, and V. J. Minkiewicz, Phys. Rev. 157, 396 (1967).

[6]G. Shirane, J. D. Axe, J. Harada, and J. P. Remeika, Phys. Rev. B 2, 155 (1970).

[7]A. S. Barker, Jr., Phys. Rev. 145, 391 (1966).

[8]Y. Yamada, G. Shirane, and A. Linz, Phys. Rev. 177, 848 (1969).

[9]J. Harada and G. Honjo, J. Phys. Soc. Japan 22, 45 (1967); G. Honjo, S. Kodera, and N. Kitamura, *ibid.* 19, 351 (1964).

[10]R. Comes, M. Lambert, and A. Guinier, Solid State Commun. 6, 715 (1968); 7, 305 (1969).

[11]A. Hüller, Z. Physik 220, 145 (1969).

[12]A. Linz, V. Belruss, and C. S. Naiman, J. Electrochem. Soc. 112, 60C (1965).

[13]M. DiDomenico, Jr., S. H. Wemple, S. P. S. Porto, and R. P. Bauman, Phys. Rev. 174, 522 (1968).

[14]S. H. Wemple, M. DiDomenico, Jr., and I. Camlibel, J. Phys. Chem. Solids 29, 1797 (1968).

[15]A. Pinczuk, W. Taylor, E. Burstein, and I. Lefkowitz, Solid State Commun. 5, 429 (1967).

[16]L. Rimai, J. L. Parsons, J. T. Hickmott, and T. Nakamura, Phys. Rev. 168, 623 (1968).

[17]D. Berlincourt and H. Jaffe, Phys. Rev. 111, 143 (1958).

[18]M. J. Cooper and R. Nathans, Acta Cryst. 23, 357 (1967).

[19]J. Harada, J. D. Axe, and G. Shirane (unpublsihed).

[20]J. D. Axe, J. Harada, and G. Shirane, Phys. Rev. B 1, 1227 (1970).

[21]A. Pinczuk, E. Burstein, and S. Ushioda, Solid State Commun. 7, 139 (1969).

[22]A. R. Hutson and D. L. White, J. Appl. Phys. 33, 40 (1962).

[23]V. Dvorak, Phys. Rev. 167, 525 (1968).

[24]M. Born and K. Huang, *Dynamical Theory of Crystal Lattices* (Clarendon, Oxford, England, 1962), Chap. V; P. B. Miller and J. D. Axe, Phys. Rev. 163, 924 (1967).

[25]W. Cochran, Advan. Phys. 18, 157 (1969).

Spin-Wave Spectrum and Magnon Contribution to the Specific Heat of EuTe

Fred Masset and J. Callaway

Department of Physics and Astronomy, Louisiana State University, Baton Rouge, Louisiana 70803

(Received 13 July 1970)

Measurements of the specific heat of EuTe at low temperatures are analyzed in conjunction with results of antiferromagnetic resonance experiments to determine first- and second-neighbor exchange parameters $J_1 = (0.07 \pm 0.02)$ °K and $J_2 = -(0.21 \pm 0.02)$ °K.

I. INTRODUCTION

Europium telluride is a fcc (rocksalt structure) antiferromagnetic insulator at low temperatures ($T_n = 9.81$ °K). The magnetic structure is of type II.[1] Antiferromagnetic resonance experiments have

shown that the spins are confined to the (111) planes with a weak preference for (11$\bar{2}$)-type directions.[2] Some lattice distortion occurs below T_n; however, the amount has not been determined and is probably small. Exchange parameters have been estimated; J_1 (nearest neighbor) being approximately 0.03 °K